CHEMICAL ENGINEERING TRANSACTIONS
VOL. 46, 2015
A publication of AIDIC
The Italian Association of Chemical Engineering
Online at www.aidic.it/cet
Guest Editors: Peiyu Ren, Yancang Li, Huiping Song

ISBN 978-88-95608-37-2; **ISSN** 2283-9216
DOI: 10.3303/CET1546165

Electronic Structure and Optical Properties of Al-doped ZnO from Hybrid Functional Calculations

Qiang Fan[a], Jianhui Yang*[a], You Yu[b], Jianping Zhang[a], Jin Cao[a]

[a] School of Physics and Electronic Engineering, Leshan Normal University, Leshan, 614004, P. R. China,
[b] College of Optoelectronic Technology, Chengdu University of Information Technology, Chengdu, 610225, P. R. China.
yjh20021220@foxmail.com

The electronic structure and optical properties of Al-doped ZnO with different concentration in wurtzite phase have been systematically investigated using the Heyd-Scuseria-Ernzerhof (HSE06) hybrid density functional on the basis of density functional theory (DFT). The calculated results show that the lattice parameters change little with Al-doped. The optical band gap and electrical conductivity gradually increase with the increasing of Al doping concentration. In addition, the Al-doped ZnO creates shallow donor states around Fermi level in the conduction band minimum from mainly Al-3s state. The dielectric function, absorption coefficient are predicted. The results show that the absorption peaks of Al-doped ZnO have a blue-shift compared with pure ZnO. Beside this, the absorption of visible light can be enhanced.

1. Introduction

Zinc oxide (ZnO) is a unique semiconductor material with a direct wide band gap (~3.40 eV) and has a large exciton binding energy (~60 meV) at room temperature, which was confirmed (Srikant and Clarke (1998), Pearton, et al. (2003)). As a result, ZnO has been widely studied for potential applications, such as chemical and gas sensors, optical and magnetic memory devices, UV-light emitting diodes, solar cells, transparent conductive oxides and some other applications, which were confirmed (Saoud, et al. (2015), Franklin, et al. (2013), Pearton, et al. (2005)). Al-doped ZnO has attracted a lot of attention due to it is a cheap, environmental friendly, more abundant, and highly stable material. The Al-doped ZnO have wide potential applications as transparent conductive oxide and electrical conductivity, Devi, et al. (2015) reported, potential solar cell electrodes, Kumarakuru, et al. (2014) reported, optoelectronic and photonic devices, Al-Ghamdi, et al. (2014) reported.
The reliable optical property is decided by accurate electronic structure. Band gap is very challenging for first principle theory, since most methods, including local density approximation (LDA) and generalized gradient approximation (GGA), the common exchange–correlation functional in the density functional theory (DFT), sometimes underestimate band gap by as large as 3 eV which was confirmed (Ruan, et al. (2014)). In this paper, we are presenting a detailed investigate for Al-doped ZnO on the electronic structure, thermodynamic stability and optical properties using the Heyd-Scuseria-Ernzerhof (HSE06) hybrid functional based on DFT rather than the scissors operator for standard DFT functional, to obtain accurate and reliable optical properties for Al-doped ZnO system.

2. Method of calculation

All calculations in our work were performed based on the DFT within the projector augmented wave (PAW) method as implemented in the Vienna Ab-initio Simulation Package (VASP) code, Kresse and Furthmuller (1996), Kresse (1999) reported. The structure optimization was performed using the GGA of DFT employing Perdew–Burke–Ernzerhof (PBE) functional form, Perdew, et al. (1997) reported. The electronic structures and optical properties were calculated on the optimized structures using the hybrid density functional HSE06, which replaces the slowly decaying long-ranged part of the Fock exchange, by the corresponding density functional counterpart. The resulting expression for the exchange-correlation energy is given by:

Please cite this article as: Fan Q., Yang J.H., Yu Y., Zhang J.P., Cao J., 2015, Electronic structure and optical properties of al-doped zno from hybrid functional calculations, Chemical Engineering Transactions, 46, 985-990 DOI:10.3303/CET1546165

$$E_{XC}^{HSE} = aE_X^{HF,SR}(\omega) + (1-a)E_X^{PBE,SR}(\omega) + E_X^{PBE,LR}(\omega) + E_C^{PBE} \quad (1)$$

where, the screening parameter ω defines the range-separation of the electron–electron interaction into a short-(SR) and long- ranged (LR) part, is assigned a value of 0.207Å^{-1}, which is called HSE06, Krukau, et al.(2006) reported. The short-range interactions become negligible when the distance exceeds 2/ω. Hartree-Fock mixing constant α is set to 0.375 for pure and Al-doped ZnO systems, Zhou, et al. (2015) reported.
The valence electron for the O, Zn and Al atoms were chosen as $2s^22p^4$, $3d^{10}4s^2$ and $3s^23p^1$, respectively. All the coordinates of atoms and the lattice parameters of wurtzite $Zn_{1-x}Al_xO$ (x=3.125%, 6.25% and 12.5%) were fully relaxed before calculating electronic structure. The electron wave function was expanded in plane waves to a cutoff energy of 500 eV with total energy converging to lower than 1×10^{-5} eV/atom. The lattice constants and all atomic positions for each supercell were fully relaxed until the maximal force on each atom was less than 0.02 eV/Å. The convergence threshold for self-consistent field (SCF) calculation accuracy was 1×10^{-6} eV/atom. A grid of 11×11×7 k points was used for the unit cell. To simulate various Al doping concentration, three different ZnO supercell (2×2×4, 2×2×2 and 2×2×1) were considered, in which one Zn atom was substituted with one Al atom, which correspond to the doping concentration 3.125%, 6.25% and 12.5%, respectively. Monkhorst-Pack grids of 3×3×1, 5×5×3, 4×4×5 were used for Brillouin zone sampling for doping concentration 3.125%, 6.25% and 12.5%, respectively.

3. Results and discussion

3.1 Structural properties

The optimized lattice constants are a = 3.257 Å and c = 5.224 Å for pure ZnO, which are in good agreement with the experimental data (a = 3.250 Å, c = 5.207 Å), Xu, et al. (2004) reported, and theoretical data (a = 3.254 Å, c = 5.238 Å), Zhou (2015) reported. The result shows that the calculation parameters are reasonable. Based on the optimized wurtzite ZnO unit cell, lattice parameters for $Zn_{1-x}Al_xO$ (x=3.125%, 6.25% and 12.5%) have been optimized as in Table 1. It is observed from Table 1, the lattice parameters change nonlinearly with the increasing of Al doping concentration and the lattice parameters of Al doping change little comparing with pure ZnO. The reasons for deviations in lattice parameters are mainly related to the little difference in the Al^{3+} (0.54 Å) and Zn^{2+} (0.74 Å) ionic radius and electro negativity between the Al and Zn atoms.

Table 1: Optimized lattice parameters of $Zn_{1-x}Al_xO$.

	x = 0	x = 3.125%	x = 6.25%	x = 12.5%
a (Å)	3.257	3.288	3.284	3.279
b (Å)	3.257	3.288	3.284	3.279
c (Å)	5.224	5.306	5.309	5.292

3.2 Electronic properties

The calculated band structures of pure ZnO along higher symmetry directions in the Brillouin zone using HSE06 hybrid functional are shown in Fig. 1. The calculated band structure shows that ZnO is a direct band gap semiconductor because the top valence and the bottom conduction are found at the same Γ point. The calculated band gap of pure ZnO is 3.31 eV, which is in excellent agreement with experimental result, Devi (2015) reported and previous calculated results of HSE06 functional form, Wan, et al. (2011) reported, and larger than the previous reported DFT results, Zhang, et al. (2012) reported. HSE06 hybrid functional solves the well-known “gap program” intrinsic factor of DFT due to adequately flexible to precisely reproduce both the potential exchange-correlation energy and equivalent potential.

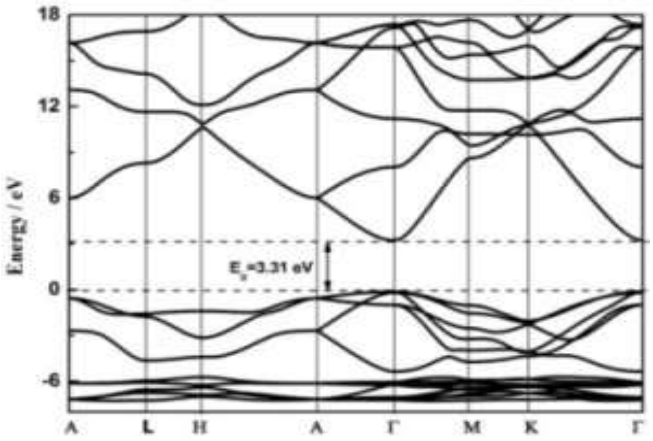

Figure 1: The band structure of pure ZnO using HSE06 hybrid functional. The Fermi level is set to 0 eV.

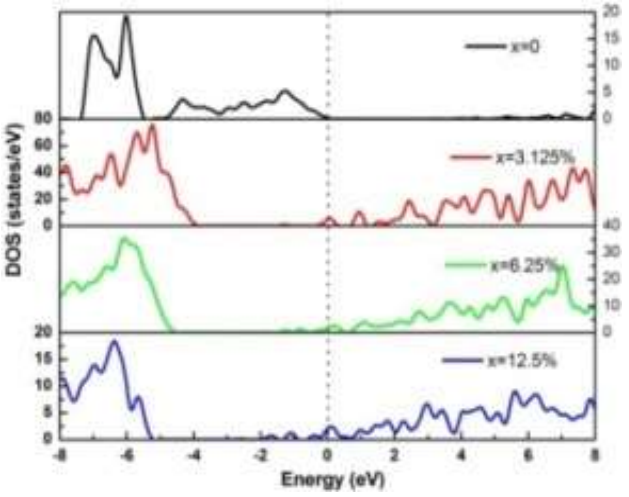

Figure 2: Total densities of states for Zn1-xAlxO (x = 0, 3.125%, 6.25%, 12.5%) using HSE06 hybrid functional. The Fermi level is set to 0 eV.

In order to show the effect of doping concentration on the electronic properties, the total densities of states (DOS) of ZnO with different Al doping concentration are shown in Fig. 2.
As shown in Fig. 2 for Al-doped ZnO, the whole energy bands move toward to the low energy region. Moreover, the shift of the energy levels increases with the increasing Al doping concentration. Compared with pure ZnO, the most remarkable feature is that the Fermi level shifts into the conductional band minimum for Al doping cases, moreover, the shift of Fermi level increases with the increasing Al concentration, which indicates a typical n-type doping behavior which was confirmed (Li, et al. (2011)). The peaks near the Fermi level become weaker and wider as Al doping concentration increases. As the increasing of Al concentration, the magnitude of these occupied states increases, the occupied states increases implies that the optical band gap (E_g* from the top of the valence band to the Fermi level) increases using Burstein-Mott-effect, Burstein (1954) reported, which were confirmed (Devi (2015), Park, et al. (2015)). Estimated optical band gap energies of 3.125%, 6.25% and 12.5% Al-doped ZnO are 3.80, 4.54 and 5.22 eV respectively.

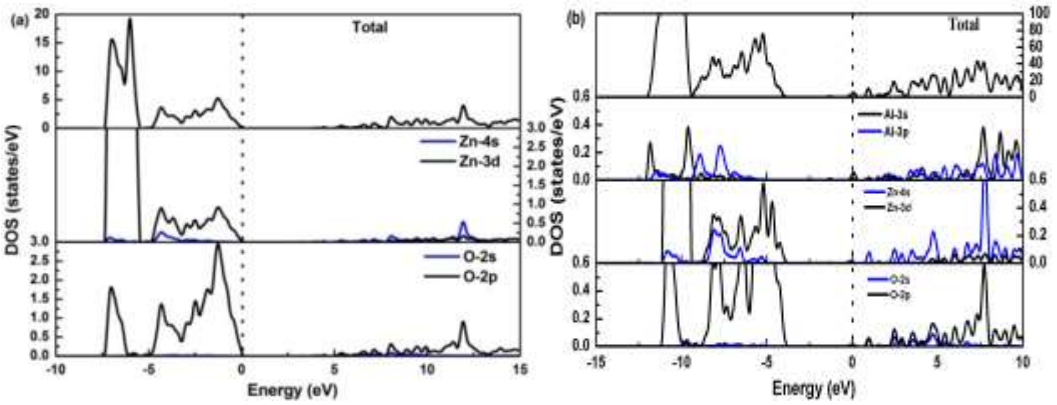

Figure 3: Partial densities of states for $Zn_{1-x}Al_xO$ at concentration x of (a) 0, (b) 3.125% using HSE06 hybrid functional. The Fermi level is set to 0 eV.

To illustrate why the optical band gap change with Al doping, we investigate the partial density of states (PDOS) for $Zn_{1-x}Al_xO$ at concentration x = 0 and 3.125% using HSE06 hybrid functional as shown in Fig. 3.
As shown in Fig. 3(a), for pure ZnO, the lower valence band (between −7.4 and −5.5 eV) is chiefly contributed by the Zn-3d states and the upper valence band (between −4.8 and 0 eV) is mainly from O-2p states. The Zn-3d states located mainly in the energy range between −7.4 and −5.5 eV, which were confirmed (Powell, et al. (1971), Maldonado and Stashans (2010)). The conduction band mainly originates from the Zn-4s states which strongly hybridize with O-2p states and has a slight contribution from Zn-3d states.
For 3.125% Al doping concentration, the whole energy bands move 4.7eV towards the low energy region. The PDOS of Zn-4s and O-2p states of Al-doping ZnO shift to lower energy range compared with those of pure ZnO. The lower valence band is mainly dominated by the contribution of Zn-3d, O-2p and mix with Al-3s states, while the upper part, near the Fermi level, is occupied by the O-2p state. Al-doped ZnO creates shallow donor states of Al-3s around Fermi level in the conduction band minimum. The conduction band upper the Fermi energy level, is primarily dominated by Zn-4s, O-2p slightly hybridize with the Al-3s, Al-3p states. The doubly occupied states is prevented by Pauli principle and therefore, the valence electrons is excited to higher energy level in the conduction band with required extra energy.

3.3 Optical properties

The optical properties can be calculated by the complex dielectric function $\varepsilon(\omega)=\varepsilon_1(\omega)+i\varepsilon_2(\omega)$, where $\varepsilon_1(\omega)$ and $\varepsilon_2(\omega)$ are the real and imaginary parts of the dielectric function, respectively. In general, the electronic band structure is directly associated with imaginary part $\varepsilon_2(\omega)$ and it can be calculated by adding all possible occupied states to the unoccupied states of transitions. Since ZnO film usually grows along the (001) orientation, the polarization vectors of incident light are set perpendicular to the c axis ($E \perp c$) in this work. The imaginary part of the dielectric function $\varepsilon_2(\omega)$ of the pure ZnO, and Al doped ZnO for different composition is shown in Fig. 4 with energy up to 10 eV.

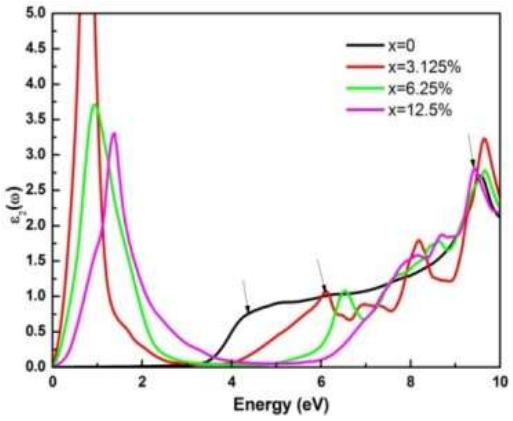

Figure 4: The imaginary part of dielectric function from HSE06 hybrid functional for $Zn_{1-x}Al_xO$ (x = 0, 3.125%, 6.25%, 12.5%) in (001) direction.

For pure ZnO, there are two main peaks at 4.41, 9.55 eV, which was confirmed (Zhou (2015)). Compared with pure ZnO, the imaginary parts $\varepsilon_2(\omega)$ of Al-doped ZnO have obvious peaks in low energy region, which originate mainly from the transitions of impurity Al-3s, Al-3p states and Zn-4s states in the conduction band, which was confirmed (Luo, et al. (2014)). On the other hand, compared with the two main peaks of pure ZnO, the corresponding peaks for Al doped ZnO shift upward energy region because the optical band gap increase with Al doped.

For the promising applications in optoelectronic devices, the optical absorption from near IR to UV region should be taken into account. The absorption coefficient $\alpha(\omega)$ can be derived from $\varepsilon_1(\omega)$ and $\varepsilon_2(\omega)$ using the relations as follows.

$$\alpha(\omega)=\sqrt{2}\omega\left[\sqrt{\varepsilon_1^2(\omega)+\varepsilon_2^2(\omega}-\varepsilon_1(\omega)\right]^{1/2} \quad (2)$$

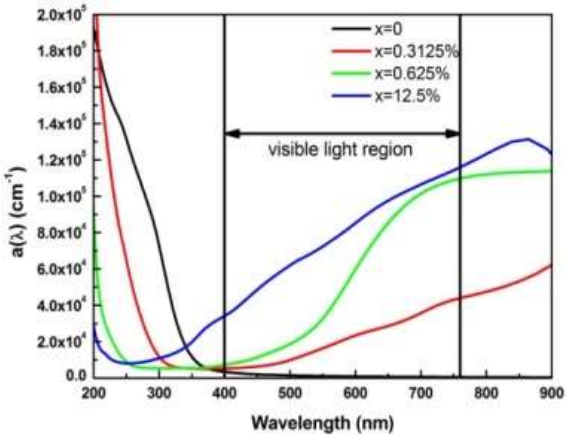

Figure 5: The absorption coefficients for $Zn_{1-x}Al_xO$ (x = 0, 3.125%, 6.25%, 12.5%) in (001) direction.

The absorption coefficients of Al doped ZnO are plotted in Fig. 5. The absorption coefficient for pure ZnO is low in the visible region, which was confirmed (Park (2015)). In UV region, the absorption coefficient decreases with increasing Al doping concentration, while in near IR region, the absorption coefficient increases with increasing Al doping concentration. Moreover, the UV absorption edge is blue shifted with increasing of Al doping concentration, due to the occupied states close to conductional band minimum are shallow donor states and the broadening of the optical band gap.

4. Conclusions

In this work, cThe results show that HSE06 hybrid functional appropriately corrects the shortcomings of standard PBE approximation for band structure. The analysis reveals that the lattice parameters of Al-doped ZnO change nonlinearly with the increasing of Al doping concentration, and the lattice parameters change little comparing with pure ZnO. The electronic structures show that the Fermi level of Al-doped ZnO shift up to conduction band, which indicates an n-type ZnO with good electrical conductivity can be obtained by Al doping. Meanwhile, the optical band gap is gradually increased with the increasing of Al doping concentration. The DOS calculations show that Zn-3d and O-2p states dominated the central and lower part of the valence band, and Al-3s states contribute to the lower part of the valence band. Al-doped ZnO creates shallow donor states of Al-3s around Fermi level in the conduction band minimum. The calculated optical properties indicate Al-doped ZnO induce a transition in the conduction band in low energy region, and absorption peaks of Al-doped ZnO have a blue-shift compared with pure ZnO. Meanwhile, Al-doped ZnO can enhance the absorption of visible light. That is to say, the Al-doped ZnO can be chosen as potential optoelectronic device applications.

Acknowledgments

We thank the financial supports from the Scientific Research Foundation of the Education Department of Sichuan Province, China (No.15ZA0273), Leshan Normal University Research Program, China (No. Z1273), Science and Technology Bureau of Leshan city, China (No.15GZD111, 15GZD113) and the National Natural Science Foundation of China (No. 51201111).

References

Al-Ghamdi A.A., Al-Hartomy O.A. and El Okr M., 2014, Semiconducting properties of Al doped ZnO thin films, Spectrochimica Acta Part A: Molecular and Biomolecular Spectroscopy, 131, 512-517, doi: 10.1016/j.saa.2014.04.020.

Burstein E., 1954, Anomalous Optical Absorption Limit in InSb, Phys. Rev., 93, 632-633, doi: 10.1103/PhysRev.93.632.

Devi V., Kumar M. and Shukla D.K., 2015, Structural, optical and electronic structure studies of Al doped ZnO thin films, Superlattice Microst, 83, 431-438, doi: 10.1016/j.spmi.2015.03.047.

Franklin L., Ekuma C.E. and Zhao G.L., 2013, Density functional theory description of electronic properties of wurtzite zinc oxide, J Phys Chem Solids, 74(5), 729-736, doi: 10.1016/j.jpcs.2013.01.013.

Kresse G., 1999, From ultrasoft pseudopotentials to the projector augmented-wave method, Phys Rev B, 59(3), 1758-1775, doi: 10.1103/PhysRevB.59.1758.

Kresse G. and Furthmuller J., 1996, Efficient iterative schemes for ab initio total-energy calculations using a plane-wave basis set, Phys. Rev. B Condens Matter, 54(16), 11169-11186, doi: http://dx.doi.org.proxy.library.stonybrook.edu/10.1103/PhysRevB.54.11169.

Krukau A.V., Vydrov O.A. and Izmaylov A.F., 2006, Influence of the exchange screening parameter on the performance of screened hybrid functionals, J Chem Phys, 125(22), 224106, doi: 10.1063/1.2404663.

Kumarakuru H., Cherns D. and Collins A.M., 2014, The growth and conductivity of nanostructured ZnO films grown on Al-doped ZnO precursor layers by pulsed laser deposition, Ceram Int, 40, 8389-8395, doi: 10.1016/j.ceramint.2014.01.045.

Li P., Deng S.H. and Li Y.B., 2011, Aluminum and nitrogen impurities in Wurtzite ZnO: first-principles studies, Physica B, 406, 3125-3129, doi: 10.1016/j.physb.2011.03.079.

Luo J., Liu Q. and Yang L., 2014, First-principles study of electronic structure and optical properties of (Zr–Al)-codoped ZnO, Comp Mater Sci, 82, 70-75, doi: 10.1016/j.commatsci.2013.09.021.

Maldonado F. and Stashans A., 2010, Al-doped ZnO: Electronic, electrical and structural properties, J Phys Chem Solids, 71(5), 784-787, doi: 10.1016/j.jpcs.2010.02.001.

Park H., Chung K. and Park J., 2015, Electronic structure of conducting Al-doped ZnO films as a function of Al doping concentration, Ceram Int, 41, 1641-1645, doi: 10.1016/j.ceramint.2014.09.102.

Pearton S.J., Norton D.P. and Ip K., 2003, Recent progress in processing and properties of ZnO, Superlattice Microst, 34(1-2), 3-32, doi: 10.1016/S0749-6036(03)00093-4.

Pearton S.J., Norton D.P. and Ip K., 2005, Recent progress in processing and properties of ZnO, Prog Mater Sci, 50(3), 293-340, doi: 10.1016/j.pmatsci.2004.04.001.

Perdew J.P, Burke K. and Ernzerhof M., 1997, Generalized Gradient Approximation Made Simple [Phys. Rev. Lett. 77, 3865 (1996)], Phys Rev Lett, 78, 1396, doi: 10.1103/PhysRevLett.78.1396.

Powell R.A., Spicer W.E. and Mcmenamin J.C., 1971, Location of the Zn 3d States in ZnO, Phys Rev Lett, 27(2), 97-100, doi: 10.1103/PhysRevLett.27.97.

Ruan X.X., Zhang F.C. and Zhang W.H., 2014, First-principles study on electronic structure and optical properties of In-doped GaN, J Theor Comput Chem, 13(08), 1450070, doi: 10.1142/S0219633614500709.

Saoud F.S., Plenet J.C. and Henini M., 2015, Band gap and partial density of states for ZnO: Under high pressure, J Alloy Compd, 619, 812-819, doi: 10.1016/j.jallcom.2014.08.069.

Srikant V. and Clarke D.R., 1998, On the optical band gap of zinc oxide, J Appl Phys, 83(10), 5447, doi: 10.1063/1.367375.

Wan R., Zhang H. and Peng J., 2011, All-electron hybrid functionals wurtzite ZnO bandgap calculations, Chem Phys Lett, 513(1-3), 17-19, doi: 10.1016/j.cplett.2011.07.068.

Xu C.X., Sun X.W. and Dong Z.L., 2004, Zinc oxide nanodisk, Appl Phys Lett, 85(17), 3878-3880, doi: http://dx.doi.org/10.1063/1.1811380.

Zhang H., Tao Z. and Xu W., 2012, First-principles study of dopants and defects in S-doped ZnO and its effect on photocatalytic activity, Comp Mater Sci, 58, 119-124, doi: 10.1016/j.commatsci.2012.01.016.

Zhou W., Liu Y. and Guo J., 2015, Electronic structure and optical properties of V- and Nb-doped ZnO from hybrid functional calculations, J Alloy Compd, 621, 423-427, doi: 10.1016/j.jallcom.2014.10.022.